Development of Magnetic Reluctance Actuators for Vibration Excitation

Daniel Wiedemann[1,a], Ulrich Koch[2,b], Heinz Ulbrich[3,c]
[1]Institute of Applied Mechanics, Technische Universität München, Munich, Germany
[2]BMW Group, Munich, Germany
[3]Institute of Applied Mechanics, Technische Universität, Munich, Germany
[a]wiedemann@amm.mw.tum.de, [b]koch@amm.mw.tum.de, [c]ulbrich@amm.mw.tum.de

Abstrac: The development and application of electromagnetic reluctance actuators for vibration excitation are presented. Main advantages are a compact and robust design with low thermal losses. The paper proposes a polarized actuator topology and describes the design procedure. An analytical method based on magnetic networks allows for a fast determination of machine parameters. finite element computations are carried out for a detailed magnetic circuit design. The combination of both methods leads to a straightforward development process for controlled reluctance actuators.

Keywords: Reluctance Actuator, Magnetic Circuit Design, Magnetic Equivalent Network, Finite Element Analysis, Vibration Excitation

Introduction

The presence of irritating noises inside the passenger compartment of vehicles has a direct influence on the perception of product quality. Particularly annoying are buzz, squeak and rattle (BSR) sounds resulting from the contact of adjacent parts. The reduction of masking noises due to the powertrain, engine and airflow raises the demands on a low noise cockpit. The emergence of silent hybrid and full electric cars will accelerate this trend considerably

To improve the noise behavior, automotive manufacturers operate vibration test rigs for the simulation of real world road drives. During road drives the vertical acceleration on the car, which causes the noise generating vibrations, is measured. Afterwards the road acceleration profile is tracked on a car test rig in the laboratory. Vibration testing during development and production avoids tedious test drives and allows for cost savings. Furthermore the car can be screened for irritating noise without interfering environmental sound, which represents an essential advantage compared to road test drives.

Conventional test rigs are based on hydraulic actuators or electrodynamic voice coil drives (shakers) for vibration excitation [1]. However, these systems have several drawbacks such as a comparatively large installation size and the need for auxiliary equipment like hydraulic power units and cooling fans [1,2]. These drawbacks and the implicated costs confine the industrial acceptance and an extensive application in the mass production of cars.

To avoid these limitations, an electromagnetic shaker system based on reluctance actuators is developed. Together with partners from the automotive industry test rigs using a twin- and quadshaker configuration were realized [3,4], see Fig.1. This paper focuses on the design of linear reluctance force actuators for the controlled tracking of acceleration profiles. We propose a polarized actuator topology. A simplified model combined with an analytical design procedure allows for a systematic actuator development. In addition, a finite element model is used to refine the magnetic circuit design. The use of both models enables an efficient actuator design.

Fig. 1: Car vibration test rigs with magnetic reluctance actuators: Twin-shaker configuration (left), quad-shaker configuration (right, actuators located on intermediate floor). Pictures courtesy of VW AG and BMW Group.

Actuator Topology

In contrast to electrodynamic shakers, which use Lorentz forces on current-carrying conductors, the actuator is based on the reluctance principle according to

$$F = \frac{\Phi^2}{2\mu_0 A}, \tag{1}$$

where Φ denotes the magnetic flux, A the armature surface and μ_0 the magnetic constant. Fig 2 shows the topology of the reluctance shaker. The polarized device realizes a linear, bidirectional motion with an amplitude of ±3.5 mm and forces up to 8 kN in neutral position. Measurements on a vibration test rig indicated, that a stroke of 4 mm and force of 5 kN are already sufficient for realistic road simulation for a passenger car [4]. The armature consists of two disks connected by the actuator shaft.

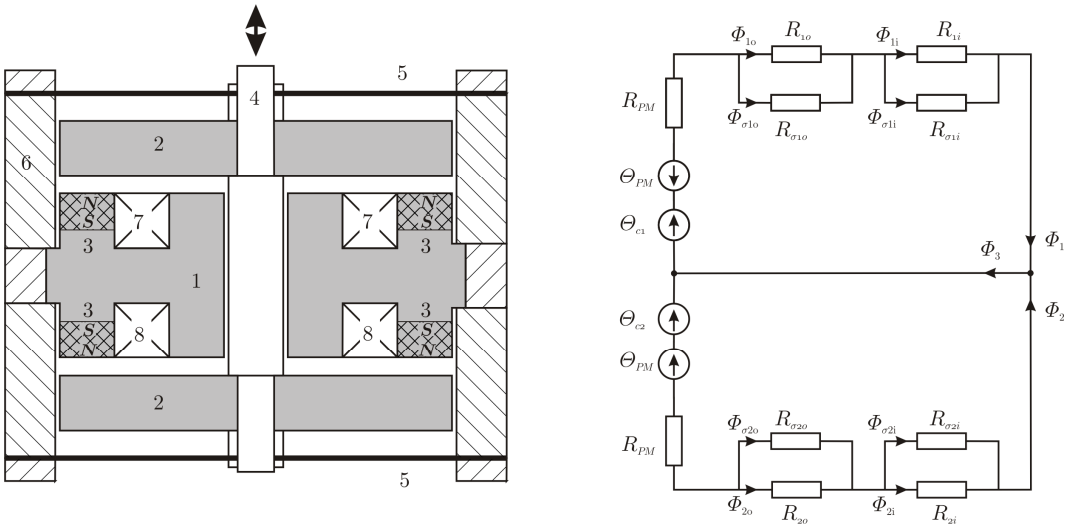

Fig. 2: Actuator topology (left) and magnetic equivalent network (right): core 1, armature 2, permanent magnets 3, shaft 4, diaphragm springs 5, casing 6, coils 7, 8.

Both, coils and permanent magnets are used as magnetomotive force sources. Actuation is achieved by superposition of coil flux and permanent magnetic flux, so that one disk of the moving iron armature is subject to more flux while flux in the other is compensated. The permanent magnetic bias enables a high force density and low heat generation. Thus, a silent operation without any disturbing cooling fan is achieved, which is crucial for noise-sensitive BSR analyses.

A thorough selection of magnetic materials is necessary to avoid eddy current influence and realize a high dynamic magnetic core. In [4] different options for eddy current avoidance are reviewed and evaluated for the present application. Radial laminations are complex and expensive. Hence, based on its good eddy current suppression and cost effectiveness, an axial lamination with shaft-parallel SiFe sheets is chosen. To meet the demands on a compact design, high energy rare-earth magnets (NdFeB) are selected. The position of the permanent magnets in the main flux path poses a risk to the long-term performance of the magnets. Thus the resistance against temperature or current induced demagnetization is another important selection criterion.

Strong armature springs allow for the stable tracking of high frequency acceleration profiles [4,5]. Here diaphragm springs combine the guidance of the shaft with the suspension. A comparison with other spring-guidance designs shows clear advantages such as low friction, stick-slip avoidance, small construction volume and customizable spring characteristics. These properties are particularly beneficial for the present application with respect to the high frequency operation at small stroke ranges.

Overall, magnetic reluctance actuators are compact, robust and low-cost drives for shaker applications. Peripherals such as cooling fans or hydraulic power units can be omitted. Thus they represent an interesting alternative compared to conventional hydraulic or electrodynamic moving coil actuators for the considered test rigs.

Magnetic Circuit Design

As a first step in the magnetic circuit design process, an analytical model based on magnetic equivalent networks (MEN) is set up. Lumped parameter models allow for a simple parameter variation and feature a low computational cost, hence they are ideal for calculation of the required reluctance surface and magnetomotive force [6,7]. Fig. 2 shows the basic reluctance network used for the dimensioning of the reluctance actuator. The magnetic circuit is considered as linear and the following assumption are made:

- the system is in neutral position, i.e. armature displacement $x = 0$
- the permanent magnets generate half of the permitted magnetic induction $B_{\max}$
- superposition of the magnetomotive force (MMF) of coils and permanent magnets: for positive maximum coil MMF $\Theta_{c,max}$ the lower working airgap is fully magnetized with B_{max}, while the upper airgap is nearly flux-free. In that case the device generates the maximum positive force F_{max}. For a reversed force a negative coil MMF is imposed.

Both, coils and permanent magnets are modeled as MMF sources. The latter has ampere turns that obey

$$\Theta_{PM} = NI_{PM} = H_c l_{PM}\,, \tag{2}$$

where H_c is the coercive field intensity and l_{PM} is the length of the permanent magnet in direction of the magnetization. Only the reluctance and leakage of the working air gaps are considered

$$R_{j,k} = \frac{x_j}{\mu_0 A_k}, \quad R_{\sigma\, j,k} = (1/\sigma - 1) R_{j,k} \qquad \text{with } j = \{1,2\}, k = \{i,o\}\,. \tag{3}$$

Here x_j denotes the airgap length, A_k the relevant armature surface and σ the leakage factor. The reluctance of soft magnetic segments of the flux path and saturation is neglected. This approach yields straightforward linear equations.

Starting with the max. magnetic force F_{max}, the required armature surface area per airgap (two airgaps per flux path) is calculated from (1) as

$$A \geq \frac{1}{2} \frac{2\mu_0 F_{\max}}{((1-\sigma)B_{\max})^2} . \tag{4}$$

For the configuration of the MMF sources the operating point of the magnetic circuit is set to $B_{max}/2$, which yields

$$\Phi_{1,\max}\big|_{\Theta_{PM}=0} = \frac{B_{\max}}{2} A = \Phi_{1,\max}\big|_{\Theta_{C1}=0} . \tag{5}$$

Equ. (5) gives the required ampere turns for the coils and the length of the permanent magnets. Introducing the vector of MMF sources $\boldsymbol{\Theta}$, the reluctance matrix $\underline{\mathbf{R}}(\mathbf{x})$ and the flux vector $\boldsymbol{\Phi}$, the resulting magnetic force is finally derived by solving the describing equation system

$$\boldsymbol{\Theta} = \underline{\mathbf{R}} \cdot \boldsymbol{\Phi} \tag{6}$$

of the magnetic network for the unknown fluxes $\Phi_{j,k}$ (cf. Fig. (2)). Subsequently the magnetic force is denoted by

$$F_{mag} = F_{mag\,2} - F_{mag\,1} = \frac{\Phi_{2i}^2 + \Phi_{2o}^2}{2\mu_0 A} - \frac{\Phi_{1i}^2 + \Phi_{1o}^2}{2\mu_0 A} \tag{7}$$

with respect to the two working airgaps of the lower und upper armature disk.

Finite Element Model

The lumped parameter model leads to satisfying results for a fast computation of the actuator dimensions. However, nonlinear material properties and leakage cannot be easily incorporated using analytical methods. With the finite element (FE) approach a nonlinear electromagnetic field computation can be carried out and thus phenomena such as saturation are included. In contrast to solid cores with a rotationally symmetric design, the axially laminated core results in a cubic actuator topology. In order to consider the underlying geometry, a three-dimensional FE model of the actuator is build using commercial software. Fig. 3 shows the geometry and the associated 3D FE discretization.

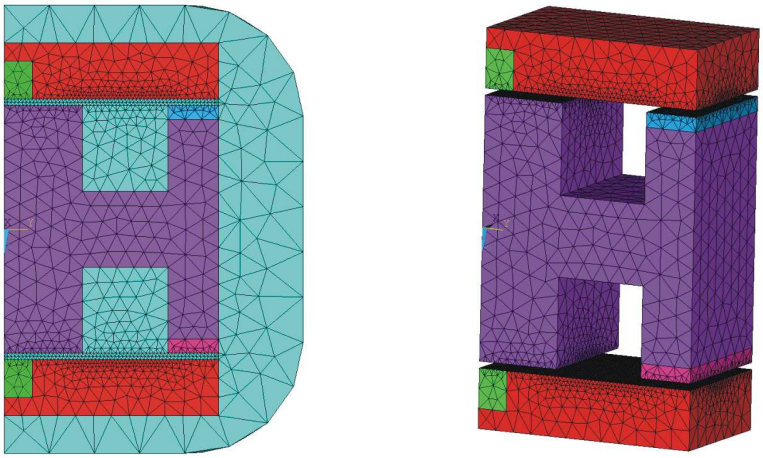

Fig. 3: Actuator geometry and associated FE discretization, quarter model: lateral view (left) and 3D profile (right).

The magneto-static model allows for simulation of all important system parameters such as force, co-energy and inductance as a function of armature position and coil current. Based on the co-energy values a dynamic model for the simulation of trajectory tracking properties of the actuator

can be derived [8]. The material properties of the permanent magnets and the nonlinear magnetization curve of the core material are included. All relevant geometrical dimensions are parameterized, which simplifies the comparison of different configurations.

Fig. 4 illustrates the computed magnetic flux density distribution for two different operating points.

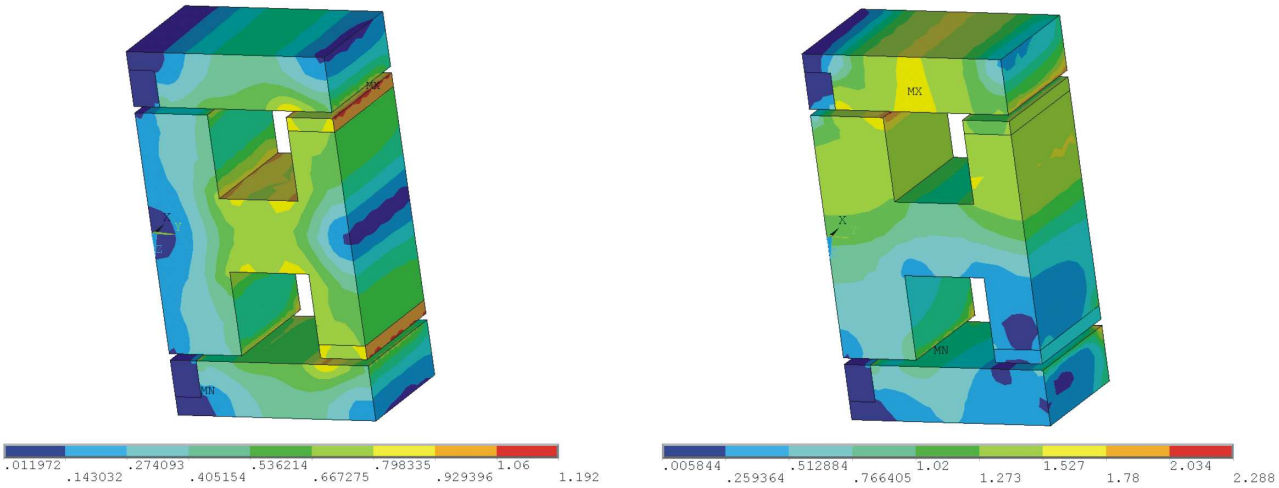

Fig. 4: Computed magnetic flux density distribution B [T] for a 3D quarter model of the reluctance actuator.
left: x = 0 mm, Θ = 0 A, F_{mag} = 0 N right: x = 0 mm, Θ = -7300 A, F_{mag} = -8021 N

In both cases the armature is in neutral position, i.e. the armature displacement x is zero. If no coil MMF is imposed, the resulting magnetic force is zero due to the symmetric design of the shaker. Based on the magnetic circuit, the required force in each armature position is achieved by superposition of coil and permanent magnet MMF, which results in the case of Fig. 4 (right) in an increased flux in the upper path and flux cancellation in the lower path. Hence a negative force and resulting armature movement is generated. However, due to the position of magnets directly at the airgaps and close to the armature, there is still a remaining flux in the non-active path.

Design Analysis

Based on the physics of the reluctance principle, the resulting force is a nonlinear function of excitation Θ and armature position x. Fig. 5 illustrates the computation results using the methods described in the previous two sections. A comparison of the magnetic force calculated from the equivalent network in (6,7) and the FE model shows a good correlation within the modeling framework. Deviations arise mainly due to the explicitly neglected saturation and leakage flux paths [9]. Hence the analytically calculated force values match well for small armature displacements and coil excitations, but at the boundaries of the operating range the analytical model deviates considerably from the numerical model. Furthermore, the assumption of complete flux cancellation in the non-active flux path does not hold anymore for large armature displacements and high coil currents. The remaining flux in the non-active segment of the magnetic circuit weakens the force development. However, the simplified model is sufficient for the determination of the actuator geometry. Using the numerical model in addition, the described more complex phenomena can also be analyzed correctly.

Conclusion

The application of electromagnetic actuators in vibration test rigs is presented. They exhibit favorable properties compared to hydraulic or electrodynamic shakers for the considered application, where high forces and small strokes are required.

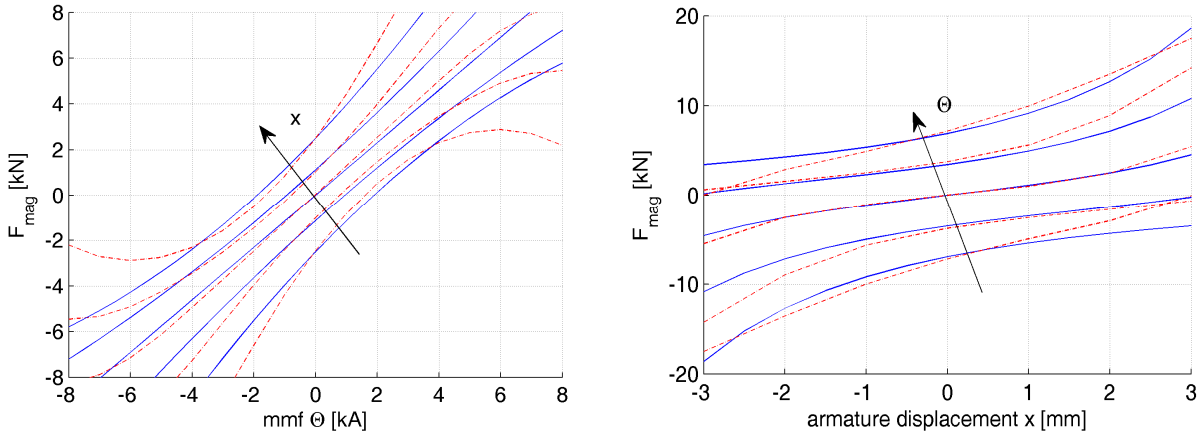

Fig. 5: Computed magnetic F_{mag} force values of the reluctance actuator. Analytical model (—), numerical model (– –). Armature displacement x = {-2,-1,0,1,2} mm, magnetomotive force (per coil) Θ={-6, -3, 0, 3, 6} kA.

Thus an actuator based on reluctance forces is proposed. Key features are a polarized and fully laminated design as well as strong armature springs for a stable and energy-efficient operation. An analytical design procedure based on magnetic equivalent networks enables the systematic actuator development. This approach neglects complex effects such as saturation and leakage to yield a straightforward approach. Thus a fast computation of different actuator geometries is feasible. However, for a more detailed simulation a nonlinear 3D FE model is used. The comparison of both models shows good correspondence, such that the simplified model is sufficient for the calculation of the actuator geometry.

References

[1] C. Harris and A. Piersol, Eds., *Harris' Shock and Vibration Handbook*, 5th ed. McGraw-Hill, 2002

[2] G. Lange and D. Snyder, *Understanding the physics of electrodynamic shaker performance*, Sound and Vibration, vol. 35, no. 10, pp. 24-33, October 2001

[3] U. Koch , D. Wiedemann and H. Ulbrich, *Model-Based MIMO State-Space Control of a Car Vibration Test Rig with Four Electromagnetic Actuators for the Tracking of Road Measurements*, IEEE Trans. Ind. Electron., 2010, to appear

[4] D. Wiedemann, U. Koch and H. Ulbrich, Linear Reluctance Actuator for Controlled Vibration Excitation, Proc. ACTUATOR 10, Bremen, Germany, 2010

[5] B. Lequesne, *Fast-acting, long-stroke solenoids with two springs*, IEEE Trans. Ind. Appl., 1990, vol. 26, no. 5, pp. 848-856

[6] J. Brauer, *Magnetic Sensors and Actuators*. IEEE Press, A John Wiley & Sons, 2006

[7] E. Kallenbach et al., Elektromagnete: Grundlagen, Berechnung, Entwurf und Anwendung, 2nd ed. Stuttgart Leipzig Wiesbaden, Germany: B.G. Teubner, 2003

[8] D. Wiedemann, U. Koch and H. Ulbrich, *A Co-Energy based Macromodel for an Electromagnetic Actuator*, Proc. IEEE Electric Machines and Drives Conf. (IEMDC), Miami, USA, 2009

[9] Ch. Chillet and J.-Y. Voyant, *Design-oriented analytical study of a linear electromagnetic actuator by means of a reluctance network*, IEEE Trans. Magn., 2001, vol. 37, no. 4, pp. 3004-3001